A Mouse Model for Slowly Progressive Primary Tuberculosis

T. MUSTAFA*†‡, S. PHYU*‡, R. NILSEN*†, R. JONSSON‡ & G. BJUNE*§

**Centre for International Health, †Department of Odontology, ‡Broegelmann Research Laboratory, University of Bergen, Bergen, Norway, and §Department of International Health, University of Oslo, Blindern, Oslo, Norway*

(Received 9 March 1999; Accepted in revised form 18 May 1999)

Mustafa T, Phyu S, Nilsen R, Jonsson R, Bjune G. A Mouse Model for Slowly Progressive Primary Tuberculosis. Scand J Immunol 1999;50:127–136

The progression from primary *Mycobacterium tuberculosis* infection to disease is usually slow in humans. The aim of this study was to develop and characterize a mouse model for slowly progressive primary tuberculosis, using the intraperitoneal (i.p.) route of infection, and to compare it with our previously described model of latent *M. tuberculosis* infection. B6D2F1 hybrid mice inoculated with 1.5×10^6 colony-forming units (CFUs) of *M. tuberculosis* H37Rv were followed-up for 70 weeks. Lungs, livers and spleens were examined for bacillary growth, histopathological changes and mycobacterial antigens (MPT64, ManLAM and multiple antigens of *M. tuberculosis*), by immunohistochemical staining. The infection was found to pass through three distinctive phases. During phase 1, mice were healthy despite development of small granulomas and an increasing number of bacilli in the lungs. During phase 2, mice were unwell but mortality was low. The count of *M. tuberculosis* and the granuloma size stabilized. The granulomas contained an increasing population of large, vacuolated macrophages. During phase 3, mice became moribund and died rapidly, but the *M. tuberculosis* count remained relatively stable. The inflammatory infiltrates filled ≈80% of the lung parenchyma and the lesions were not well demarcated. Rapidly progressing inflammation, rather than an increase in the *M. tuberculosis* count, seems to contribute more to mortality.

Dr Tehmina Mustafa, Centre for International Health, Armauer Hansen building, Haukeland University Hospital, N-5021 Bergen, Norway

INTRODUCTION

After infection with *Mycobacterium tuberculosis* in humans, ≈90% of the infected individuals mount a protective immune response and remain clinically well, the only evidence of infection being development of a positive tuberculin test. In ≈10% of the infected individuals, the infection will progress to disease [1,2]. The progression of primary infection to disease is slow in humans. It is estimated that the majority (≈80%) of infected individuals who develop disease will do so within the first 2 years of infection [2–5]. As it is only a small proportion of infected individuals who develop clinical disease, the risk factors for infection may be quite different from the risk factors for clinical disease following infection. Most of the studies in experimental models in mice have focused on rapidly progressive disease after inoculation with a high dose of *M. tuberculosis* [6,7], or treatment with antituberculosis drugs (after initial infection and renewed infection) to study memory immune response [8]. There are recent studies on slowly progressive infection in lungs, by infecting the mice via intravenous (i.v.) [9,10] and aerosol [11] routes.

We have previously established mouse models for latent tuberculosis (TB) and rapidly progressive primary disease by using the intraperitoneal (i.p.) route of infection [12]. After i.p. injection, inert substances, radioactive materials, proteins and bacteria are absorbed quickly (within 2 h in the case of bacteria), drain first to the mediastinal lymph nodes and reach the lungs of rat within 24 h [13–17]. The bacilli thus injected i.p. will initially reach mediastinal lymph nodes, resembling natural airborne infection. Airborne infection is undoubtedly the most appropriate route of infection for mimicking human TB in an animal model. It is, however, difficult to obtain complete control over the desired dosage in mice when giving TB bacilli by the aerosol route [18]. Bacilli that are trapped in the fur will be licked and ingested, stimulate the gut-associated lymphoid tissue and modify the immune response. Infection of mice by aerosol also poses a hazard to the researchers, and it is necessary to have sophisticated and expensive facilities [19].

The aim of this study was to develop and characterize a mouse model to study the natural course of slowly progressive disease after primary infection using the i.p. route, and to compare this model clinically, bacteriologically and histopathologically with our previous models of latent infection and rapidly progressive disease [12]. In our latent infection model, a low-to-moderate dose ($4\times10^1-4\times10^5$ bacilli) is given i.p. The mice do not develop clinical disease or obvious pathology over a long period of time and present no spontaneous reactivation of disease. The number of *M. tuberculosis* bacilli (measured in colony-forming units [CFUs]) is found to stabilize in the lung and spleen after week 26. In the rapidly progressive disease model, infection with a high dose (10^8) of bacilli gives a higher bacterial count in the lungs, rapid development of disease, early mortality and no recovery [12]. In the model of slowly progressive primary TB, when 1.5×10^6 bacilli were given, the number of bacteria stabilized in the lungs and spleens after week 20, but the mice progressed slowly from subclinical infection to disease, and later to morbidity and mortality.

MATERIALS AND METHODS

Mice. B6D2F1Bom (C57BL/6JBom × DBA/2JBom) female mice were purchased from Bomholtgård Breeding and Research Centre Ltd (Ry, Denmark). All mice were ≈ 12 weeks of age at the start of the experiments. The average lifespan of these mice is 975 days. Animal care was as described previously [12]. The experiments were performed with the permission of the Norwegian Experimental Animal Board, and Norwegian Law corresponds with the European Convention on the Protection of Experimental Animals.

Bacteria. All experiments were conducted with the H37Rv strain of *M. tuberculosis*. The stock bacillary suspension was prepared as described previously [12]. Two hundred microlitres of phosphate-buffered saline (PBS) containing $\approx 1.5\times10^6$ CFU of *M. tuberculosis* were inoculated i.p. into each mouse.

Experimental design. A total of 260 mice were infected. Six uninfected mice were kept, as sentinel controls, in cages with the infected mice. No cross-infection was observed. Ten uninfected control mice were kept under the same conditions as the infected mice, but in a separate isolator, as controls for growth and age-related changes. Mice were killed at 1, 2, 4 weeks and then at 4-weekly intervals up to week 41 and later at 52, 57 and 70 weeks after infection. At each time-point, mice were selected at random, but at week 57, comparatively healthier mice (eight mice) were selected.

Processing specimens for bacillary counts. A detailed procedure for processing lungs, liver and spleen for bacillary counts has been described previously [12]. Until week 24, one lung, one-half of spleen and liver were analysed, from each mouse, for bacillary counts. From week 29 onwards, both lungs, whole spleen and liver were analysed from each mouse. Ten-fold serially diluted tissue homogenates were plated on Middlebrook 7H10 medium (Difco Laboratories, Detroit, MI, USA). The plates were incubated at 37 °C, in an atmosphere of 5% CO_2. The reading of CFUs was discontinued when the counts remained unchanged for three consecutive weeks. The maximum time the culture plates were kept was 3 months after inoculation.

Tissue preparation for histopathology. One lung was fixed by immersing one-half of it in 4% phosphate-buffered formaldehyde (pH. 7.3), and the other half was frozen in isopentane prechilled with liquid nitrogen. From week 29 onwards, perfusion of the lungs followed by fixation was performed. The left lung was perfused with 4% buffered formalin, fixed and embedded in paraffin. The right lung was perfused with a mixture (1 : 1, v/v) of distilled water and Tissue-Tek (OCT compound, Leica Mikroscopi AS, Oslo, Norway) before freezing. The frozen specimens were embedded in OCT compound and stored at − 70 °C until sectioning.

For histological analysis, two 5-μm thick sections from each specimen were cut at 100-μm intervals, placed on the same glass slide and stained with haematoxylin and eosin (H & E).

For detection of fibrosis, Sirius red stain for connective tissues was used [20]. In brief, after hydration and washing in running water for 10 min, sections were stained in 0.1% picro-Sirius red F3BA, in saturated aqueous picric acid solution, for 30 min (Sirius red F3BA-Jurr; BDH, Laboratory Supplies, Poole, UK). After dehydration, tissues were cleared in xylene and mounted.

Histological evaluation. The total area of a section and the area of section occupied by the focal inflammatory infiltrates (granulomas) and extensive inflammatory infiltrates after week 40 were measured. The area of granuloma was measured in a Leitz Dialux 22 EB microscope with × 1 and × 10 objective lens connected to a Sony CCD video camera using the image-processing system Videoplan (Kontron Bild-analyse, Eching, Germany). The total area of the section was measured by projecting the sections onto paper using a projector (Carl Zeiss, Jena, Germany) at a magnification of × 17. The drawings were measured on the digitizer after calibration of the system using the image-processing system. The degree of inflammation was determined by a 'granuloma fraction' (GF).

$$\mathrm{GF} = \frac{\text{Area of inflammatory infiltrate}}{\text{Total area of the lung section}}$$

The area of inflammatory infiltrate was the granulomas and extensive inflammatory infiltrates measured after week 40. The GF was calculated for two sections from each mouse. At each time-point, the mean GF for three to four mice was calculated.

Detection of mycobacterial antigens. Mycobacterial antigens were detected by immunohistochemistry. The antibodies used were:

(1) anti (a)-MPT64, a polyclonal antibody reacting with a secreted protein isolated from the early *M. tuberculosis* culture fluid [21,22];

(2) a-ManLAM, a polyclonal antibody reacting with mannose-capped lipoarabinomannan, a cell wall component from *M. bovis*, bacillus Calmette–Guérin (BCG) Copenhagen strain [23,24]; and

(3) a-BCG, a polyclonal antibody reacting with multiple antigens of sonicate and culture fluid of *M. bovis* BCG Copenhagen strain (Dako A/S, Copenhagen, Denmark) [25,26].

M. bovis BCG and *M. tuberculosis* are extensively similar in their antigenic content [27]. Anti-BCG is expected to react with multiple antigens of *M. tuberculosis*. The antigens detected by a-BCG were designated as mycobacterial antigens.

Formalin-fixed paraffin-embedded tissues were studied for the presence of mycobacterial antigens. The fixation process leads to formation of complex aldehyde-linked protein aggregates in which primary and secondary protein structures might be preserved, while the tertiary or quaternary protein structures are altered by extensive cross-linking. Therefore the accessibility of antigenic epitopes might be limited. Such hindrances may be partially reversed by retrieval techniques like enzyme digestion and microwave oven heating [28–30]. To identify a suitable method for antigen retrieval, the effect of pretreatment with enzyme and microwave oven heating was studied in tissues from eight mice in the following three experiments:

(1) enzyme pretreatment, where tissues were treated with 0.1% trypsin in tris phosphate-buffered saline (TBS) for 10 and 20 min;

(2) microwave pretreatment, where slides were placed in citrate buffer solution, pH 6.0 (Dako A/S), and heated in a microwave oven (Miele electronic M696, Germany) for 5 and 10 min at 700 W; and

(3) a combination of enzyme and microwave pretreatments.

From these experiments, enzyme pretreatment for 20 min was found to give the best results for antigen retrieval.

Frozen tissues were studied for the detection of MPT64, ManLAM and mycobacterial antigens at the time-points shown in Table 1.

The immunohistochemical method of staining has already been described [12]. Briefly, the formalin-fixed paraffin-embedded sections were deparaffinized and treated with the enzyme before incubation, while the frozen sections were fixed in cold acetone for 10 min. Endogenous peroxidase activity was blocked with H_2O_2. Sections were also pretreated with avidin and biotin-blocking solution in order to reduce endogenous biotin staining (Vector Laboratories, Burlingame, AL, USA). To block nonspecific binding mainly with Fc receptors, incubation was carried out using swine serum. Sections were then incubated overnight with primary antibody. Incubation with biotinylated swine antirabbit immunoglobulin G (Dako A/S) followed by incubation with avidin–biotin–peroxidase complex (ABC; Dako A/S) was carried out. Location of antigen was visualized by incubating sections with H_2O_2 and 3-amino-9-ethylcarbazol-containing buffer. The sections were washed in TBS between each incubation. The slides were counterstained slightly with Mayer's haematoxylin. As a negative control, 1% bovine serum albumin (BSA)/TBS was used instead of primary antibody.

Evaluation of immunostaining. For the evaluation of mycobacterial antigen load, three to four mice were analysed at each time-point. The antigen-containing cells were enumerated by light microscopy as:

(1) total number of antigen-positive cells/mm^2 of the lung tissue from each mouse. The whole lung section was counted; and

(2) percentage of mycobacterial antigen-positive cells, evaluated using a $\times 40$ ocular fitted with a 10×10 mm graticule. The antigen-positive cells and the total number of nucleated cells were counted for each field. For each specimen, three to four fields were counted from the inflammatory area.

Survival analysis. Late in the experiment, the mice were moribund. To reduce their suffering, these moribund mice were killed after week 47 according to a fixed set of exclusion criteria, as it was observed that mice fulfilling these criteria died within 24–48 h. Seven characteristics, namely body form (normal—thin cachectic), spine form (normal—lordosis or kyphosis), appearance of coat (flat—raised pelt), gait (flat—toeing), activity (active—passive), behaviour (running—immobile) and abdominal muscles (flat abdomen—guarding) were used. Each characteristic was given a score of 5 to 1, according to severity, 1 being the worst. Mice that had a score of 1 in four characteristics, including cachexia, were considered moribund and were killed. These killed mice were considered as spontaneously dead. Among 143 dead mice, 24 deaths occurred between weeks 40 and 47 and were not recorded by exact dates. These deaths were distributed equally over these weeks.

Statistical analysis. For survival analysis the Kaplan–Meier model was used [31]. This analysis was performed using the software program SPSS (SPSS, Inc., Chicago, IL, USA). This is a method of estimating time-to-event models in the presence of censored cases.

The Mann–Whitney *U*-test was used for two-group comparisons. Statistical significance was defined as a P-value < 0.05.

RESULTS

Clinical status of mice

Mice stayed healthy until week 16 after infection. Thereafter, the mice started developing signs of illness. Between weeks 20–40 the mice were unwell, but mortality was low. By week 30, 7% of the mice had died. Around week 40, the majority of mice became moribund and started dying rapidly. Figure 1 shows the survival curve for the whole observation period. The last death recorded was in week 70. The remaining 16 mice were killed at weeks 70 and 74.

Lungs

As evaluated using gross pathology, the lungs appeared normal until week 4 after infection. At weeks 8 and 12 the killed mice had pink, air-containing lungs of normal size, speckled with grey lesions varying in number and size but always relatively small. At week 16, one or two whitish-yellow nodules per lung appeared besides grey-black small nodules. From week 20 onwards, the nodules were whitish-yellow surrounded by a greyish-blue zone, and were harder than the surrounding lung tissue. The nodules increased in number and size. At week 37 the nodules appeared smaller, more like the nodules from the week 20 specimens. However, in one mouse, most of the lung tissue was whitish-yellow, hard and consolidated by confluence of the nodules. After week 41, the nodules were all confluent, merging into larger whitish-yellow and hard areas.

The GF (as defined in the Materials and methods) is shown in Fig. 2. The granulomas increased in size with progression of time from week 4 until week 16. From week 20 until week 37, the granuloma size remained relatively unchanged. From week 37 to week 41 there was a sudden increase in granuloma size, filling $\approx 80\%$ of the lung sections; it then remained quite stable for the rest of the experimental period.

One and two weeks after infection, there was diffuse infiltration of inflammatory cells in the alveolar-capillary interstitium in some areas of the lung parenchyma, as observed using light microscopy. The cells were mainly lymphocytes and macrophages, together with a few polymorphonuclear cells (PMNs). The blood vessels in the interstitium were dilated. The alveolar spaces did not contain any inflammatory cells. After week 4, the lungs showed focal infiltrates of inflammatory cells (granulomas). The granulomas were small and contained predominantly macrophages and lymphocytes. A few PMNs were also present. The lymphocytes and PMNs were usually seen around blood vessels as well as distributed in the whole granuloma (Fig. 3A,B). These early granulomas, where the macrophages were mixed with the lymphocytes, were categorized as mixed granulomas (MG). At week 4, all the infiltrates were MG.

With progression of time, the granulomas increased both in number and size. The distribution of macrophages and lymphocytes became more defined in the granulomas (Fig. 3C,D). The macrophages increased in size and attained a vacuolated appearance (light staining vesicular nuclei, increased vacuolated eosinophilic

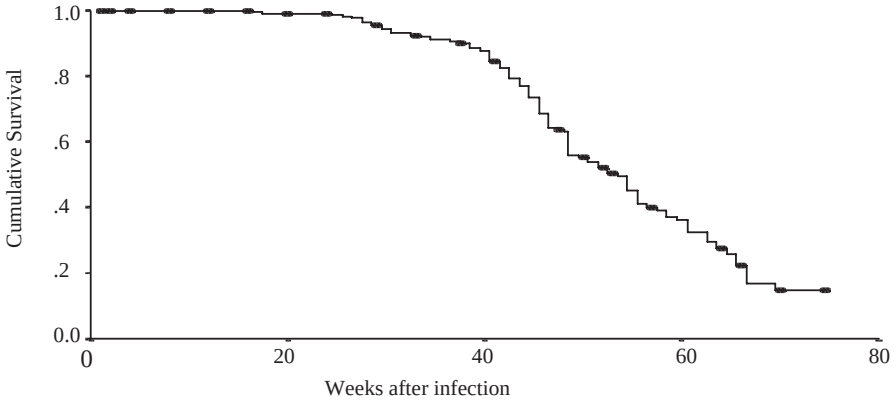

Fig. 1. Survival of mice with slowly progressive primary tuberculosis. Analysis was performed using the Kaplan–Meier model in SPSS. The killed mice (●) were censored from the analysis.

cytoplasm), and demonstrated a syncytial appearance. Few lymphocytes and pyknotic bodies were seen (Fig. 3D). These areas were called macrophage aggregates. The lymphocytes were initially more scattered in the granuloma, but gradually formed loose aggregates called lymphocyte aggregates. PMNs were found scattered in the macrophage and lymphocyte aggregates and more so in the vicinity of pyknotic bodies. These granulomas, with a differential distribution of macrophages and lymphocytes, were categorized as differentiated granulomas (DG). At weeks 8 and 12, the infiltrates were of both MG and DG types, with dominance of MG at week 8 and of DG at week 12. With Sirius red staining, delicate fibrils were seen in the lesions from week 12.

From week 16 onwards, all the infiltrates were of the DG type. In the macrophage aggregates, groups of degenerated cells were seen. Fibroblasts appeared around the groups of degenerated cells. Collagen and reticular fibres that were dispersed in the granulomas increased and appeared mature and thicker compared with earlier time-points. With progression of time there was an increase in the number of degenerated cells, fibrous tissue and PMNs in the macrophage aggregates. At weeks 33 and 37, in the lungs of four out of six mice the inflammatory response was focal. However, in two mice, there was an extensive spread of the inflammatory infiltrate involving ≈70% of the lung parenchyma.

From week 41 onwards, the mice exhibited a shift in the histopathology. The inflammatory infiltrates were no longer distinctly focal and there was a significant increase in the size of the inflammatory infiltrates compared with weeks 20–37 ($P = 0.0001$). Extensive diffuse inflammatory infiltrates occupied 70–80% of the lung parenchyma (Fig. 2 & Fig. 3E). This increase in the size of infiltrates was due to an increase in the number of vacuolated macrophages. The lymphocyte aggregates were reduced in size (Fig. 3E,F). The number of fibroblasts was increased but there was no significant increase in the collagen and reticular fibres compared with weeks 20–37. After week 40, the majority of the mice were moribund but some mice were less unwell. At week 57, the less unwell mice were killed. At week 70, because of the killing and death of moribund mice, the less unwell mice were selected. The moribund mice at weeks 41 and 52 had focal areas of cellular debris (Fig. 3G). These areas fused to form large foci of necrosis (Fig. 3H). There were markedly few lymphocytes. The bronchiolar lumen contained the cellular debris. The mice that were less unwell had no such focal areas of cellular debris and the lymphocyte aggregates were larger than in the moribund mice.

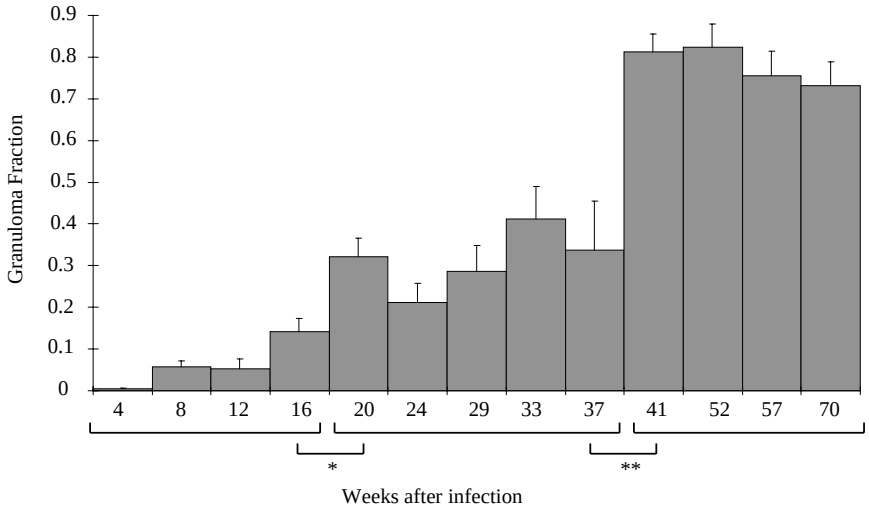

Fig. 2. Granuloma fraction (GF) in the lungs of mice with slowly progressive primary tuberculosis. The GF was defined as described in the Materials and methods. In each group, $n = 3$ or 4 mice. Bars indicate the standard error of the mean (SEM). Significant differences were observed between weeks 4–16 and weeks 20–37 ($*P = 0.0001$) and between weeks 20–37 and weeks 41–70 ($**P = 0.0001$).

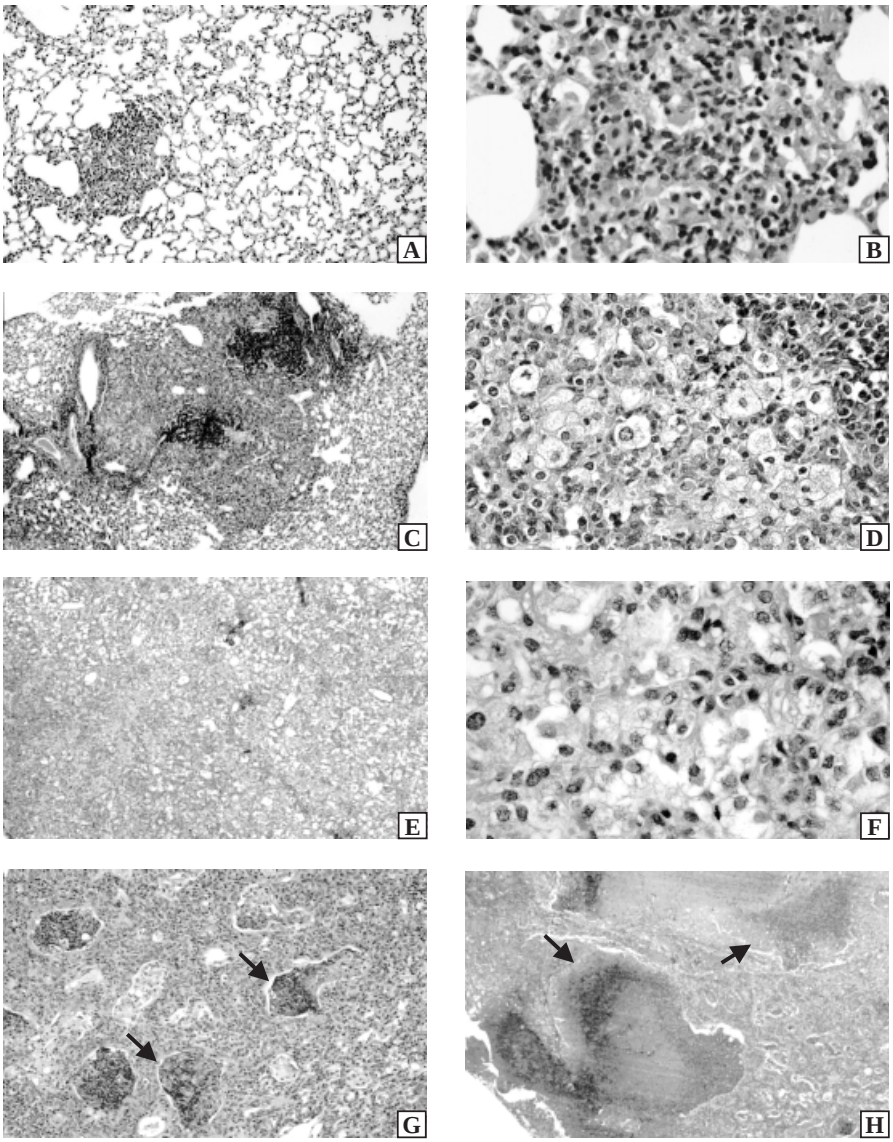

Fig. 3. Lung tissue, from mice with slowly progressive primary tuberculosis, stained with haematoxylin and eosin. (A)×104 and (B)×416, mixed granuloma 4 weeks after infection. Macrophages and lymphocytes are mixed without any differentiation. (C)×38 and (D)×400, differentiated granuloma 20 weeks after infection. (C) Distribution of macrophages and lymphocytes becomes differentiated; macrophages form syncytia and lymphocytes form loose aggregates. (D) Macrophage aggregates showing vacuolated macrophage syncytium formation. Few lymphocytes and pyknotic bodies are seen. (E–H), weeks 41–70 after infection. (E)×40 and (F)×400, the granulomas break down and the inflammatory infiltrate disperses and occupies ≈80% of the lung parenchyma. The lymphocyte aggregates are reduced. (F) The vacuolated macrophages increased in inflammatory infiltrates and lymphocytes are found individually among the macrophages. (G)×100 to (H)×40, the moribund mice at weeks 41 and 52 developed multiple foci of cellular debris. (H) The small foci fused to form large foci of necrosis.

Mycobacterial antigens in the tissues

Mycobacterial antigens were not detected in formalin-fixed lung tissue sections until week 8 after infection. Antigens were detectable only in the macrophages in the granulomatous lesions. Within different granulomas in the same lung section, the antigen distribution varied. At week 8, ≈50%, and between weeks 12 and 20, ≈75% of the granulomas contained detectable antigens. From week 24 onwards almost all the granulomas contained antigens.

Figure 4 shows the total number of mycobacterial antigen-positive cells (stained cells)/mm^2 of the lung section. The number of stained cells varied among the positively stained granulomas in the same lung section. Some granulomas contained very high numbers of stained cells compared with others, even though the size, cellular components and morphology of the granulomas were not so different. The number of stained cells was, however, not significantly different between the groups of mice, killed at each time-point, up to week 20. At weeks 24 and 29, the number of stained cells was significantly higher than at earlier time-points. At weeks 33 and 37, the number of stained cells decreased to the same level observed at week 20. At weeks 41 and 52, the moribund mice had a significantly higher number of stained cells compared with (week 57 and 70) mice that were less unwell ($P = 0.045$). The total number of stained cells varied during the course of infection but the percentage of stained cells (3–7%) remained relatively stable.

Macrophages staining positively for mycobacterial antigens seemed to contain highly variable amounts of antigen. Figures 5 and 6 show the different intensities and patterns of mycobacterial antigen staining during the course of infection. The pattern of staining was mainly granular and also sometimes diffuse. Rod-shaped particles were rarely seen. The staining intensity was recorded as weak, moderate or strong. Cells with all different intensities of staining were present at all time-points but with varying frequency. At week 8 after infection, in MG, cells

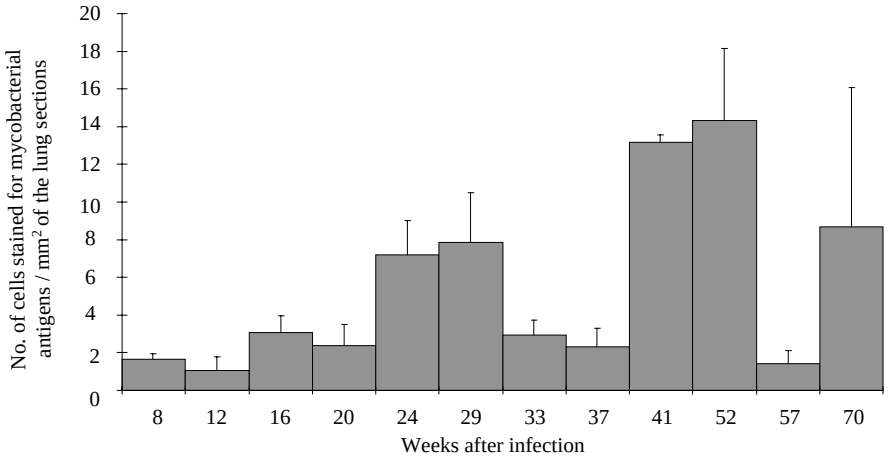

Fig. 4. Mycobacterial antigen-positive cells/mm^2 of the lung sections of mice with slowly progressive primary tuberculosis. Mycobacterial antigens were detected by immunohistochemical staining of tissue section with a-bacillus Calmette–Guérin (a-BCG) polyclonal antibody. In each group, $n = 3$ or 4 mice. Bars indicate the standard error of the mean (SEM). At each time-point mice were chosen randomly for killing, but at weeks 57 and 70 mice that were comparatively less sick were selected. After week 40, the differences between moribund (weeks 41 and 52) and less sick (weeks 57 and 70) mice were significant ($P = 0.045$).

staining with weak intensity (cells containing small and fine granules) dominated (Fig. 5A,B). As the granulomas differentiated, the vacuolated macrophages with moderate staining intensity (cells containing bigger and coarser and a higher number of granules than in weakly staining cells, but the cytoplasm was not filled with antigen as in strongly staining cells) dominated (Fig. 5C,D). From weeks 20–37, the majority of macrophages stained with moderate and strong intensity (cells were full of granules) (Fig. 5E,F). Antigen-containing cells were found either singly or in groups of 3 to 15 cells. With the progression of infection, groups of degenerating macrophages usually stained for antigens. However, some of the antigen-loaded cells, usually present singly, did not show signs of degeneration. In a granuloma, in spite of the same vacuolated appearance of all the macrophages, only $\approx 5\%$ stained for antigens. At weeks 57 and 70, in the less sick mice that had fewer antigen-containing cells, cells staining with weak and moderate intensity dominated (Fig. 6A,B), whereas the moribund mice at weeks 41 and 52 had a higher number of antigen-containing cells with predominance of moderate and strong staining intensity (Fig. 6C,D). The necrotic foci contained large amounts of antigens (Fig. 6E), and the bronchiolar lumen containing cellular debris also exhibited antigen (Fig. 6F).

Table 1 shows the MPT64, ManLAM and mycobacterial antigens detected in the frozen lung tissue. The level of all antigens increased with progression of time. Before week 40, the number of stained cells and intensity of stain for ManLAM and mycobacterial antigens was similar. At week 29 and week 41 in the moribund mice, there was a greater number of ManLAM-containing cells than mycobacterial antigen-containing cells. This could be because of an increase in the amount of ManLAM in the tissues at weeks 29 and 41. The a-ManLAM fraction in the a-BCG antiserum might not be able to detect traces of ManLAM as efficiently as the specific a-ManLAM. The number of mycobacterial antigen- and ManLAM-containing cells were higher than MPT64-containing cells at week 41. The MPT64-containing cells were present singly, as well as in small groups, whereas the ManLAM-positive cells were present mostly in groups (Fig. 6G,H).

A similar amount and pattern of mycobacterial antigens was observed in paraffin sections and in frozen sections until week 20. At weeks 24, 29 and 41, when the load of antigen was high, there was a greater number of cells containing mycobacterial and ManLAM antigens in frozen sections than in paraffin sections from the same animals. Deparaffinization of paraffin sections might have removed some of the lipids.

The livers showed no gross pathology. Microscopically, a few small foci of lymphocytes with few macrophages were seen in mice with clinically severe disease. Spleens were enlarged but did not contain detectable granulomas. Neither did the kidneys contain any detectable granulomas.

Table 1. Semiquantitative analysis of the mycobacterial antigens detected in the frozen lung sections by immunohistochemical staining

	Frozen sections		
Weeks after infection	MPT64*	ManLAM†	Mycobacterial antigens‡
8	ND	ND	+
12	ND	ND	+
16	ND	ND	+
20	+	++	+
24	++	++	++
29	ND	+++	++
41	++, +++	++++	+++
70	ND	ND	+

Mycobacterial antigens were detected by polyclonal antibodies: * a-MPT64, reacting with a secreted *Mycobacterium tuberculosis* protein; † a-ManLAM, reacting with mannose-capped lipoarabinomannan; ‡ a.-BCG, reacting with multiple antigens of *M. bovis* bacillus Calmette–Guérin (BCG). *M. bovis.* BCG and *M. tuberculosis* are extensively similar in their antigenic content, thus a-BCG is expected to react with multiple antigens of *M. tuberculosis*.

+, < 5; ++, 9–13; +++, ≈ 20; ++++, 25–40 stained cells/mm^2 of lung section.

ND, not done.

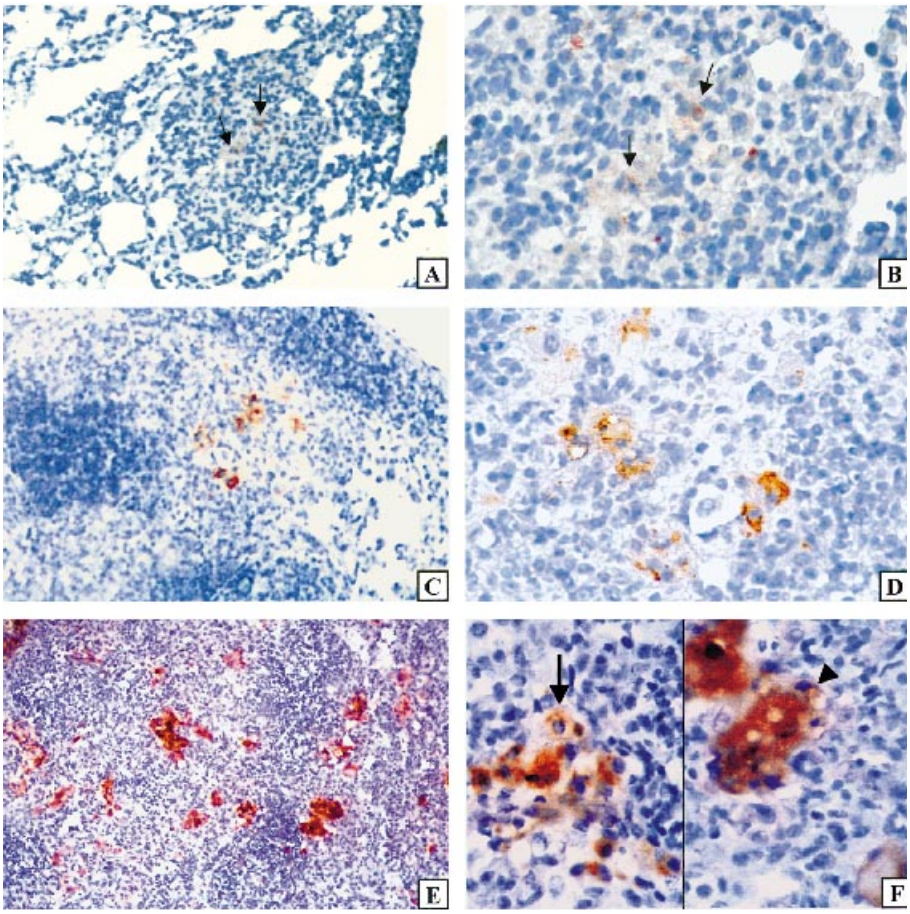

Fig. 5. Lung tissue from mice with slowly progressive primary tuberculosis showing mycobacterial antigens in formalin-fixed paraffin-embedded tissue sections stained with the avidin–biotin–peroxidase complex (ABC). The antigens were detected by using a-bacillus Calmette–Guérin (a-BCG) polyclonal antiserum. Antigens were always localized in the macrophages. (A–D), week 8 after infection: (A) ×184 and (B)×448, mixed granuloma with cells containing small and fine granular staining (weak intensity of stain); (C) ×176 and (D) × 440, differentiated granuloma containing a higher amount of antigen. Cells contain bigger and coarser granules that do not fill the whole cytoplasm (moderate intensity). (E)×101 and (F)×480, week 24 after infection: the granulomas contain a higher level of antigens compared with earlier time-points. The cells staining with strong intensity (arrow head) also appear beside those staining with moderate intensity (arrow).

Bacillary growth

Figure 7 shows the bacterial count (in CFUs) of *M. tuberculosis* in the lung, liver and spleen during the course of infection. In the lungs, at week 1 after inoculation, CFUs were the lowest among the three organs. There was a progressive increase in CFUs in the lungs until week 20. From week 20–37, the counts remained stable, although higher than the earlier time-points (weeks 1–20) ($P = 0.0001$). At weeks 41 and 52, there was a further increase in the CFUs. In less sick mice, at weeks 57 and 70, the CFUs were lower compared with the moribund mice at weeks 41 and 52 ($P = 0.0008$) and were at the same level as in the stable period of weeks 20–37.

In the spleen and liver, there was an increase in CFUs from weeks 1 to 2, and after that the CFUs gradually decreased. In the spleen after week 12, and in the liver after week 16, there was an increase in CFUs, corresponding with the time when the mice started to become unwell. Subsequently, the CFUs were stable in both organs. The CFUs in the spleen were higher than in the liver throughout the course of infection. At the end of the experiment, the CFUs in all the organs seemed to be similar to those during the stable period (weeks 20–37).

DISCUSSION

In this study we established a mouse model of slowly progressive primary TB by inoculating 1.5×10^6 bacilli i.p. and characterized it clinically, histopathologically and bacteriologically. The course of infection could be separated into three distinct phases. During the first phase, mice were clinically healthy in spite of development of small granulomas and rapid bacillary growth in the lungs. In the second phase, mice were unwell but mortality was low. The granuloma size and the CFUs remained stable. During the third phase, there was a sudden increase in mortality and morbidity and an explosive spread of inflammation in most of the lung but with no substantial increase in CFUs.

The progression from disease (phase 2) to mortality (phase 3) coincided with a shift from a focal, granulomatous host response to a diffuse extensive inflammatory infiltrate involving 80% of the lung parenchyma (Fig. 2). The bacterial count did not increase substantially with the shift to phase 3 (Fig. 7). The immune response of the host, rather than an increase in the number of bacteria, seemed to determine the progression of disease to mortality. A similar finding was made in our previous study where mice with latent infection had no obvious lesions. When these mice were challenged with corticosterone, extensive inflammatory infiltrates developed in the lungs, coinciding with disease and mortality, whereas the increase in bacterial number was not significant [12]. This model has been studied further for T-cell phenotypes and cytokines *in situ* to identify changes in the cytokine profile or T cells that coincide with a shift in

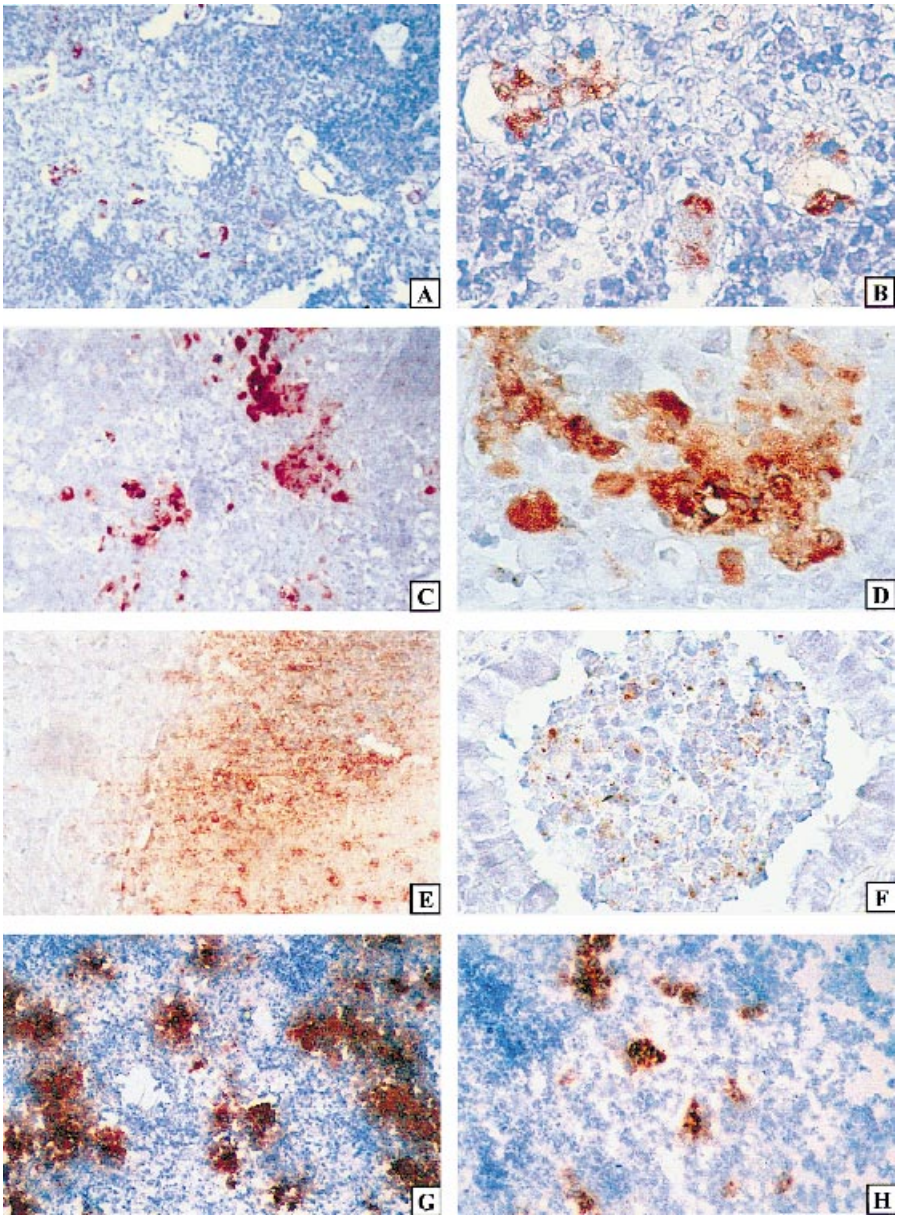

Fig. 6. Lung tissue from mice with slowly progressive primary tuberculosis showing mycobacterial antigens stained with the avidin–biotin–peroxidase complex (ABC), during weeks 41–70 after infection, in (A–F) formalin-fixed paraffin-embedded and (G–H) frozen sections. At each time-point, mice were chosen randomly for killing, but at weeks 57 and 70 mice that were comparatively less sick were selected. (A) and (B), mice that were less unwell. (A)×110, lungs had a lesser amount of mycobacterial antigen (detected by a-bacillus Calmette–Guérin [a-BCG] polyclonal antiserum) compared with the moribund mice. (B)×424, cells with a moderate intensity of stain predominated. (C–H), moribund mice. (C)×114, a greater amount of mycobacterial antigen compared with mice that were less unwell. (D)×422, cells with strong intensity of stain predominated. (E)×200, the necrotic foci contained a large amount of antigen. (F)×416, the bronchiolar lumen containing cellular debris also contained antigens. (G)×110, a very high amount of ManLAM was detected in frozen sections compared with paraffin-embedded sections. Deparaffinization of tissues might have resulted in the removal of lipids. (H)×110, the level of MPT64 (secretory *Mycobacterium tuberculosis* antigen) was less than LAM.

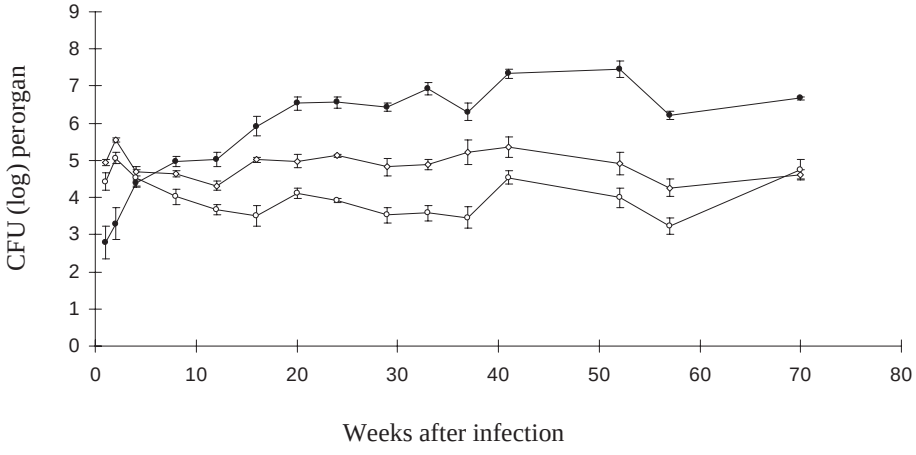

Fig. 7. Colony-forming units (CFU) of *Mycobacterium tuberculosis* in (●) lung (◇) spleen and (○) liver tissue of mice with slowly progressive primary tuberculosis. In each group, $n = 3$ or 4 mice. Bars indicate the standard error of the mean (SEM). At each time-point, mice were chosen randomly for killing, but at weeks 57 and 70, mice that were comparatively less sick were selected. After week 40, the differences in CFUs between moribund (weeks 41 and 52) and mice that were less sick (weeks 57 and 70) was significant ($P = 0.001$).

morphology of lesions (T. Mustafa, S. Phyu, R. Nilsen: manuscript in preparation).

During the third phase there was a variation in the degree to which the mice were unwell. The majority of the mice were moribund but some mice were less unwell. At weeks 57 and 70, the mice that were less unwell were selected for comparison with moribund mice at weeks 41 and 52. The moribund mice had a significantly higher level of mycobacterial antigens and bacteria in the lungs compared with the healthier mice. Some of the moribund mice had focal areas of necrosis whereas no necrotic foci were found in the mice that were less unwell, even though in both groups the lesions occupied $\approx 80\%$ of the lung parenchyma.

The clinical variations seen in mice have a resemblance to human TB where the prognosis of sputum-positive individuals varies. Without chemotherapy, 50% of the diseased individuals die, 30% are self-cured and the remaining 20% remain alive but are infectious [32,33].

Expansion of vacuolated macrophages coincided with the progression from subclinical infection to disease and from disease to mortality. Both these shifts were associated with an increase in the size of macrophage aggregates, thereby indicating at an association of vacuolated macrophages with immunopathology. From their morphological appearance, these macrophages seem to have increased secretory activity. During phase 3, the lymphocyte aggregates decreased in size, whereas there was an increase in the number of vacuolated macrophages. In the moribund mice, the lymphocyte aggregates almost disappeared and the individual lymphocytes were found scattered between macrophages. There is evidence that apoptosis of T cells from TB patients is increased compared with healthy control subjects [34]. Mycobacterial antigens were detected in only 5% of the vacuolated macrophages. Presumably these antigen-containing macrophages play a key role in providing a continuous antigen stimulus, eliciting the cytokine production leading to an expansion of the lesions.

LAM was the major antigen detected in the macrophages (Fig. 6G). LAM can deactivate macrophages by blocking the production of H_2O_2, nitric oxide and tumour necrosis factor-α (TNF-α) [35,36]. LAM can also block the activation of macrophages via interferon-γ (IFN-γ) by inhibiting the transcription of IFN-γ-inducible genes [37] and induces the release of transforming growth factor-β (TGF-β) from human monocytes [38], which deactivates the mycobactericidal functions of macrophages [39,40].

In humans, subsequent to infection there is formation of a 'primary complex' in the majority of individuals [1]. Progression of infection to disease in $\approx 10\%$ of the infected individuals [1,2] is presumably because the granulomas in these individuals are unable to contain the infection. This resembles the situation of small, mixed granulomas during the first phase of infection in our model. Further study of our model may help to understand the risk factors for progression of infection to primary disease in humans. One risk factor was the high dose of infection and, consequently, the number of bacilli initially present in the lungs. This is evident when we compare this model of slowly progressive TB with our previous models of latent infection and rapidly progressive disease [12].

The histopathological findings in our model are consistent with those of Dunn & North [9,10] and Rhoades *et al*. [11] in several regards. Fibrosis is suggested to play a key role in the pathogenesis of slowly progressive primary TB [10]. In our study, fibroblasts were present in the lesions throughout the course of infection and increased in number with the shift to phase 3. No striking increase in the collagen or reticular fibres were, however, seen with the progression of pathology in phase 3.

In conclusion, 1.5×10^6 CFU of H37Rv given i.p. to mice resulted in slowly progressive primary TB, which passed through three distinctive phases, resembling human primary TB. The first phase was characterized by subclinical infection, development of small granulomas and an increase in CFUs. During the second phase, mice developed signs of disease. The granulomas increased in size and contained more vacuolated macrophages. CFUs and granuloma size remained stable. The third phase was characterized by increased mortality and a sudden loss of the granulomatous nature of the lesions and spread of inflammatory infiltrates in most of the lung parenchyma without any substantial increase in the CFUs. The increase in morbidity and mortality appears to occur as a result of sudden changes in the host immune response, rather than because of an increase in CFUs.

ACKNOWLEDGMENTS

The authors are grateful to Dr Morten Harboe at the Institute of Immunology and Rheumatology (University of Oslo, Oslo, Norway), for providing the a-LAM and a-MPT64 antisera and for useful advice. We acknowledge Øyunn Nielsen at the Laboratory for Oral Microbiology (Faculty of Dentistry, University of Bergen) and Eirik Røynstrand at the Department of Pathology (Haukeland University Hospital) for providing technical assistance, and thank Gry Bernes and Hilda Emilia Azevedo Andersen for providing excellent technical assistance in animal care. Special thanks are given to Kathrine Skarstein for help with the image-processing system, to Rune Daniel Haakonsen for help with the photographs, to Valborg Baste for statistical advice and to Carla Olsnes for proofreading the manuscript. This study was supported by the European Commission (Grant ERBIC 18CT960060) and a research grant from the University of Bergen, Norway.

REFERENCES

1 Roger MDP, Craig RH. *Mycobacterium tuberculosis*. In: Mandell GL, Douglas RG Jr, Bennett JE, eds. Principles and Practice of Infectious Diseases. New York: Churchill Livingstone, 1990: 1877–906.
2 Styblo K. Recent advances in epidemiological research in tuberculosis. Adv Tuberc Res 1980;20:1–63.
3 Gedde-Dahl T. Tuberculosis infection in the light of tuberculin matriculation. Am J Hygiene 1951;56:139–214.
4 Sutherland I. Recent studies in the epidemiology of tuberculosis, based on the risk of being infected with tubercle bacilli. Adv Tuberc Res 1976;19:1–63.

5 Medical Research Council. BCG and whole bacillus vaccines in the prevention of tuberculosis in adolescence and early adult life. Bull WHO 1972;46:371–85.
6 Nyka W, Faherty JF, Malone LC, Kiser JS. A histological study of the pathogenesis of tuberculosis in mice experimentally infected with bacilli of human type. Exp Med Surg 1954;12:367–429.
7 Raleigh GW, Youmans GP. The use of mice in experimental chemotherapy of tuberculosis: II. Pathology and pathogenesis. J Infect Dis 1948;82:205–20.
8 Andersen P, Heron I. Specificity of a protective memory immune response against *Mycobacterium tuberculosis*. Infect Immun 1993;61:844–51.
9 Dunn PL, North RJ. Persistent infection with virulent but not avirulent *Mycobacterium tuberculosis* in the lungs of mice causes progressive pathology. J Med Microbiol 1996;45:103–9.
10 Dunn PL, North RJ. Virulence ranking of some *Mycobacterium tuberculosis* and *Mycobacterium bovis* strains according to their ability to multiply in the lungs, induce lung pathology, and cause mortality in mice. Infect Immun 1995;63:3428–37.
11 Rhoades ER, Frank AA, Orme IM. Progression of chronic pulmonary tuberculosis in mice aerogenically infected with virulent *Mycobacterium tuberculosis*. Tuberc Lung Dis 1997;78:57–66.
12 Phyu S, Mustafa T, Hofstad T, Nilsen R, Fosse R, Bjune G. A mouse model for latent tuberculosis. Scand J Infect Dis 1998;30:59–68.
13 Spencer J, Gyre LA, Hall JG. IgA antibodies in the bile of rats. III. The role of intrathoracic lymph nodes and the migration pattern of their blast cells. Immunology 1981;48:687–93.
14 Courtice FC, Simmonds WJ. Physiological significance of lymph drainage of the serous cavities and lungs. Physiol Rev 1954;34:419–85.
15 Yoffey JM, Courtice FC. Lymph flow from regional lymphatics. In: Yoffey JM, Courtice FC, eds. Lymphatices, Lymph and the Lymphomyeloid Complex. London: Academic Press, Inc., 1970: 295–9.
16 Olin T, Saldeen T. The lymphatic pathways from peritoneal cavity: a lymphoangiographic study in the rats. Cancer Res 1964;24:1700–11.
17 Buxton BH, Torrey JC. Absorption from the peritoneal cavity. J Med Res 1906;15:5–87.
18 Lefford MJ. Diseases in the mice and rats. In: Kubica GP, Wayne LG, eds. The Mycobacteria—a Source Book. New York: Marcel Dekker, 1984: 947–74.
19 Orme IM, Collins FM. Mouse model of tuberculosis. In: Bloom BR, ed. Tuberculosis: Pathogenesis, Protection, and Control. Washington, DC: ASM Press, 1995: 113–34.
20 Sweat F, Puchtler H, Rosenthal SI. Sirius Red F3BA as a stain for connective tissue. Arch Pathol 1964;78:69–72.
21 Nagai S, Wiker HG, Harboe M, Kinomoto M. Isolation and partial characterization of major protein antigens in the culture fluid of *Mycobacterium tuberculosis*. Infect Immun 1991;59:372–82.
22 Harboe M, Closs O, Bjorvatn B, Kronvall G, Axelsen NH. Antibody response in rabbits to immunization with *Mycobacterium leprae*. Infect Immun 1977;18:792–805.
23 Harboe M, Closs O, Svindahl K, Deverill J. Production and assay of antibodies against one antigenic component of *Mycobacterium bovis* BCG. Infect Immun 1977;16:662–72.
24 Venisse A, Berjeaud JM, Chaurand P, Gilleron M, Puzo G. Structural features of lipoarabinomannan from *Mycobacterium bovis* BCG. Determination of molecular mass by laser desorption mass spectrometry. J Biol Chem 1993;268:12401–11.
25 Closs O, Harboe M, Axelsen NH, Bunch-Christensen K, Magnussen M. The antigens of *Mycobacterium bovis*, strain BCG, studied by crossed immunoelectrophoresis: a reference system. Scand J Immunol 1980;12:246–63.
26 Wiley EL, Mulhollan TJ, Beck B, Tyndall JA, Freemann RG. Polyclonal antibodies raised against bacillus Calmette-Guerin, *Mycobacterium duvalii* and *Mycobacterium paratuberculosis* used to detect mycobacteria in tissues with the use of immunohistochemical techniques. Am J Clin Pathol 1990;94:307–12.
27 Wiker HG, Harboe M, Bennedsen J, Closs O. The antigens of *Mycobacterium tuberculosis*, H37Rv, studied by crossed immunoelectrophoresis. Comparison with a reference system for *Mycobacterium bovis*, BCG. Scand J Immunol 1988;27:223–39.
28 Shi SR, Key ME, Kalra KL. Antigen retrieval in formalin-fixed, paraffin-embedded tissues: an enhancement method for immunohistochemical staining based on microwave oven heating of tissue sections. J Histochem Cytochem 1991;39:741–8.
29 Shi SR, Chaiwun B, Young L, Cote RJ, Taylor CR. Antigen retrieval technique utilizing citrate buffer or urea solution for immunohistochemical demonstration of androgen receptor in formalin-fixed paraffin sections. J Histochem Cytochem 1993;41: 1599–604.
30 Mighell AJ, Robinson PA, Hume WJ. Patterns of immunoreactivity to an anti-fibronectin polyclonal antibody in formalin-fixed, paraffin-embedded oral tissues are dependent on methods of antigen retrieval. J Histochem Cytochem 1995;43:1107–14.
31 Kaplan EL, Meier P. Non parametric estimation from incomplete observations. J Am Stat Assoc 1958;53:457–81.
32 Springett VH. Tuberculosis control in Britian 1945–1970–1985. Tubercle 1971;52:136–47.
33 National Tuberculosis Institute. Tuberculosis in a rural population in South India: a five year epidemiological study. Bull WHO 1974;51:473–88.
34 Hirsch CS, Toosi Z, Vanham G *et al.* A role of apoptosis in suppressed T-cell responses in patients with tuberculosis in Uganda. Tuberc Lung Dis 1997;78:75–84.
35 Chatterjee D, Roberts AD, Lowell K, Brennan PJ, Bloom BR. Structural basis of capacity of lipoarabinomannan to induce tumour necrosis factor. Infect Immun 1992;60:1249–53.
36 Adams LB, Fukutomi Y, Krahenbuhl JL. Regulation of murine macrophage effector functions by lipoarabinomannan from mycobacterial strains with different degrees of virulence. Infect Immun 1993;61:4173–81.
37 Chan J, Fan X, Hunter SW, Brennan PJ, Bloom BR. Lipoarabinomannan, a possible virulence factor involved in persistence of *Mycobacterium tuberculosis* within macrophages. Infect Immun 1991;59:1755–61.
38 Dahl KE, Shiratsichi H, Hamilton BD, Ellner JJ, Toosi Z. Selective induction of transforming growth factor in human monocytes by lipoarabinomannan of *Mycobacterium tuberculosis*. Infect Immun 1996;64:399–405.
39 Ding A, Nathan CF, Graycar J, Derynck R, Stuhr DJ, Srimal S. Macrophage deactivating factor and transforming growth factor beta 1, 2 and 3 inhibit induction of macrophage nitrogen oxide synthesis by IFN gamma. J Immunol 1990;145:940–4.
40 Tsunawaki S, Sporn M, Ding A, Nathan C. Deactivation of macrophages by transforming growth factor β. Nature 1988;334: 260–2.